

# Optimized Design of Floating Stone Columns for Soft Soils Enhanced Long-term Settlement Performance

Chenche Khaoula<sup>a1</sup>, Bouali Meriem Fakhreddine<sup>1</sup> and Jorge Castro<sup>2</sup>

<sup>1</sup> Department of Civil Engineering, Faculty of Sciences and Technology, InfraRES Laboratory  
University of Mohamed Chérif Messaadia, Souk Ahras, Algeria

<sup>2</sup> Group of Geotechnical Engineering, Department of Ground Engineering and Materials Science,  
University of Cantabria, Avda. de Los Castros, s/n, 39005 Santander, Spain

<sup>a)</sup> Corresponding author: k.chenche@univ-soukahras.dz

## Abstract

In two-dimensional axial symmetry finite element analyses, compressible clayey deposits improved by a large group of floating stone columns were performed using the unit cell idealization, i.e., only one column and its corresponding surrounding soil. The primary focus of this study is to assess the efficiency of floating stone columns in enhancing the consolidation rate of low-permeable soft soils. Additionally, it aims to evaluate the long-term stability of constructions built along marine coastal areas, such as harbors. To this end, two real case studies were investigated; the Béjaïa and Algiers Mediterranean harbors. Within the scope of this study, the Béjaïa case presents a solid reinforced concrete foundation of a silo structure, while the Algiers case features a strip foundation, both involving significantly large loaded areas. Various geometric variables, pertaining to the design of floating stone columns, have been considered to analyze their effect in impacting the consolidation process and the long-term behavior emphasizing their fundamental importance in the design. Besides, a thorough comparison between the design, in both short-term and long-term conditions, satisfying the admissible settlement, has been made, ultimately resulting in the optimized design selected. The results also indicate that increasing both the area improvement ratio and the floating stone column length leads to a speeding up of the consolidation rate. However, in contrast to the area substitution ratio, the column length has comparatively lesser importance on the performance in terms of reducing the settlement. Importantly, it is demonstrated that the design of floating stone columns for long-term conditions is significantly distinct from that for short-term conditions, requiring an approximate 40% increase in the area improvement ratio. The reason is that designs based on the immediate settlement may not align with improved soft soil long-term behavior. Finally, the study reveals that the applied load ultimately governs the design of floating stone columns.

**Keywords:** Compressible soil; Consolidation; Floating stone column; Numerical analysis; Optimized design; Settlement; Unit cell idealization.

## Nomenclature

$A$	Influence zone cross-section	$\alpha$	Area improvement ratio
$A_c$	Total cross-section of the stone column	$\beta$	Depth ratio
$B$	Raft width	$\gamma_d$	Dry unit weight
$c_c'$	Stone column material effective cohesion	$\varphi_c'$	Stone column material drained angle of friction
$c_s'$	Initial soil effective cohesion	$\varphi_s'$	Initial soil drained angle of friction
$c_g$	Geometry-dependent constant for installation pattern	$\nu_c$	Poisson's ratio of the stone column material
$C_K$	Correction factor for the post-installation earth pressure	$\nu_s$	Poisson's ratio of the initial soil
$C_q$	Correction factor for the loading intensity	$\psi_s$	Dilation angle of the initial soil
$C_a$	Correction factor for the area improvement ratio	$\psi_c$	Dilation angle of the stone column material
$C_\varphi$	Correction factor for the friction angle		
$D_c$	Column diameter		
$d_e$	Influence zone diameter		
$E_c'$	Young's modulus of the stone column material		
$E_s'$	Young's modulus of the initial soil		
$H$	Thickness of the compressible layer		
$k$	Coefficient of permeability		
$K$	Post lateral earth pressure coefficient		
$L_c$	Column length		
$n$	Settlement improvement factor		
$n_o$	Basic improvement factor		
$q$	Applied loading		
$r_c$	Stone column radius		
$r_e$	Influence area radius		
$S_c$	Column's axis-to-axis spacing		

## 1. Introduction

Compressible soils, like clays and silts, are commonly known for their low permeability which results in slow rates of consolidation and poor water dissipation causing long-lasting excessive stability defects once loaded (e.g., [Beyene et al., 2023](#)). The need for construction over these soils remains a daunting challenge in geotechnical engineering. To successfully deal with it, the improvement with stone columns is purposely applied to reduce the settlement and accelerate the consolidation process. Its effectiveness in stabilizing and enhancing weak soils has been demonstrated by numerous research studies (e.g., [Boru, et al., 2022](#)). It significantly influences the initial soil characteristics, the overall performance, and the behavior of the improved soil ([Shehata et al., 2021](#)). Moreover, it provides a cost-effective alternative solution; compared to pile foundation, it presents a 37% cost reduction ([Bouassida and Guetif, 2007](#)). Stone columns are introduced as a set of in-situ ground improvement techniques. They consist of vertical drains filled with a well-compacted granular material, usually ballast, incorporated by a dry or wet method (e.g., [Tabchouche and Bouassida, 2020](#)).

End-bearing stone columns, i.e., fully penetrating columns resting on rigid stratum, are commonly used. Otherwise, floating stone columns can in some cases be adopted when the rigid stratum level cannot be reached. In such instances, particular attention is crucial when assessing the treatment depth (e.g., [Miranda et al., 2021](#)).

Several contributions have been suggested to predict the behavior of a large group of floating stone columns ([Van Impe and De Beer, 1983](#), [Schweiger and Pande, 1986](#), and [Mitchel and Huber 1985](#)). Among these contributions are those using the unit cell idealization. As defined, for example, by [Castro \(2017\)](#), the unit cell model is perfectly suited to analyze the settlement of end-bearing and encased groups of stone columns and its evolution as a function of time. Moreover, in the case of a group of floating stone columns, it allows the prediction of the behavior beneath the floating columns' toes due to the punching failure produced in the unreinforced underlying layer. This concept is particularly suitable for cases where a significant number of columns and a large loaded area are involved, as it leverages symmetry conditions to ensure consistent column behavior. The unit cell model has been embraced by numerous researchers in their analyses (e.g., [Castro and Sagaseta, 2011](#), [Castro et al., 2014](#), [Doan and Fatahi, 2020](#) and [Ng and Tan, 2014](#)).

[Bouassida \(2016\)](#) and [Imam et al. \(2021\)](#) both emphasize that the design of floating stone columns typically involves two key verifications satisfying bearing capacity and settlement requirements. However, particular attention should be given to the study of settlement since the backfilled material enhances the geotechnical properties of weak and highly compressible soils, thereby increasing the bearing capacity. The semi-empirical method of [Priebe published in 1976 \(Priebe, 1976\)](#), later adapted and supplemented in 1995 ([Priebe, 1995](#)), is extensively used worldwide in the design of vibro-substitutions. The so-called [Priebe's method](#) focuses on estimating the settlement of end-bearing columns given as a settlement improvement factor,  $n$ , which is the ratio between the settlement without stone columns and that with columns. This method takes into account the compressibility of the stone column and the variation of stress with depth.

As precisely pointed out by [Remadna et al. \(2020\)](#), the proper design of floating stone columns is heavily dependent on two important parameters: length and area replacement ratio. Many studies have extensively examined how geometric variables for the floating stone column design affect the performance with a particular focus on reducing settlement. For instance, [Killeen and McCabe \(2014\)](#) predicted that as the column length increases, there will definitely be a gradual decrease in settlement. They have also stated that the performance of a small group of stone columns is influenced by various parameters, such as the area replacement ratio and the number of columns, rather than the width of the footing. As per [Castro \(2017\)](#), for a small group of stone columns, the main controlling parameter of the critical length, and hence settlement reduction, is the extension of the load, i.e., the footing width.

Recently, [Beyene et al. \(2023\)](#) performed a finite element analysis, using *Plaxis*<sup>3D</sup>, of soft clay improved with a group of vertical floating drains made of highly permeable material to investigate the impact of drains dimension on the deformation response and consolidation attributes. The authors reported the effectiveness of the vertical drains in improving the permeability and minimizing the consolidation period of low-permeable soft clays. The analysis further indicates that, in the case of a triangular grid pattern, the consolidation rate remains marginally higher when compared to a square grid pattern which lasts for an extended period of time for the consolidation process to reach completion. Using the unit cell concept, [Ng and Tan \(2014\)](#) performed a two-dimensional analysis to examine the response of floating stone columns under loading. The amount of settlement and the excess pore water pressure dissipation were predicted for different area and depth replacement ratios. The authors showed that the improvement with stone columns managed to reduce the settlement as the depth and the area improvement ratios increased; subsequently, the consolidation rate accelerated. Moreover, based on the consolidation analysis results, a new simplified method is developed to estimate the settlement improvement factor of floating stone column-improved soft soil.

The present paper further examines the influence of several design parameters and the optimization of floating stone column design using real case studies. Consequently, the paper addresses short-term, consolidation and long-term settlements and their impact on a large group of floating stone columns optimized design. In light of this fact and by adopting the unit cell axis-symmetry idealization, the ongoing study, based on finite element analyses, investigates the impact of geometric parameters for floating stone column design, namely; length and area substitution ratio, on the long-term behavior with regard to the admissible drained settlement. Firstly, this paper explores the importance of considering the long-term settlement in the design of a large group of floating stone columns. It involves undrained analysis followed by consolidation analysis on a reinforced concrete foundation supporting a silo with a diameter of 58 meters treated with a group of floating stone columns at Béjaïa Harbor. The analysis included a comparison of the predicted values for both short-term settlement and settlement over time, emphasizing the crucial need to account for the long-term behavior as well as the load level in the design. Secondly, the study explores a real stone column project within the context of the consolidation works at the Port of Algiers' container terminal. This project deals with soil improvement using stone columns, allowing it to support a large uniform load distribution over a strip footing with a width of 16.38 meters. Computed settlements in both conditions are compared for various area improvement ratios and lengths, ultimately leading to the determination of an optimized design satisfying the admissible drained settlement. Ultimately, the examination of the impact of the load level is explored.

The results of the current study highlight the efficiency of floating stone columns in improving the consolidation performance of compressible soft soils. Furthermore, it is demonstrated that increasing both the area improvement ratio and the column length leads to accelerating the consolidation process of saturated soils and reducing the settlement, which is a critical factor relevant for optimizing the design of floating stone columns. To conclude, assessing the long-term deformation is essential for the proper design of a large group of floating stone columns, as designs intended for immediate settlement may not align with long-term behavior.

## **2. Numerical Investigation**

### **2.1. Simulation procedure**

The numerical analysis presented hereafter is defined using *Plaxis*<sup>2D</sup> finite element software, specially intended for analyzing deformation and stability in the domain of geotechnical engineering and rock mechanics. The present study examines the settlement response as a function of time of floating stone column-improved ground. The idealization of

the unit cell axis-symmetry has been employed. This type of modeling is suitable for simulating rafts or extensive uniformly loaded areas characterized by geometrical and loading symmetries as in the case of tanks and embankments... (e.g., Bouassida, 2016). Geometrically, this model comprises a single column situated at the center of an extensive grid of stone columns, all enclosed by a cylinder that encompasses the tributary surrounding soil (Elshazly et al., 2008). The unit cell diameter ( $d_e$ ) represents the corresponding influence zone of the column, characterized by the typical installation pattern and the axis-to-axis spacing between the columns. Using the equivalence of areas, the zone or the domain of influence of each column arrangement can be expressed as:

$$d_e = c_g S_c$$

where  $c_g$  represents the geometry-dependent constant, taking values of 1.05, 1.13, and 1.29 for triangular, square, and hexagon patterns, respectively (Balaam and Booker, 1981). Among these arrangement patterns, the triangular pattern is the most commonly employed for installing stone columns due to its larger coverage area for each individual column compared to other patterns (e.g., Nayak et al., 2019).

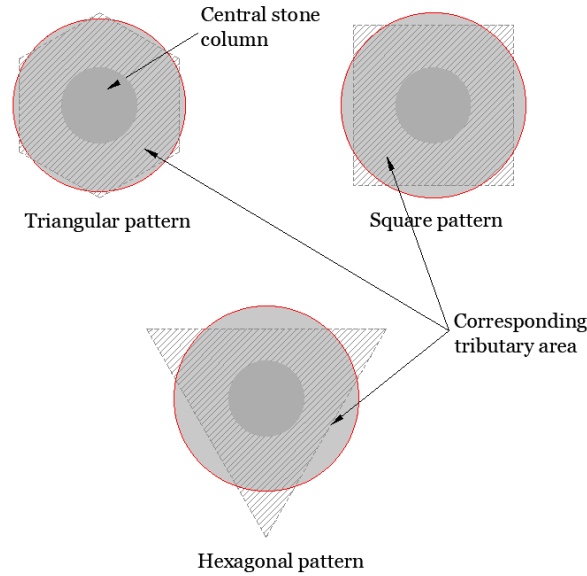


Fig. 1. Corresponding tributary area surrounding the stone column.

This analysis adopts the precise geometry and material properties of the Mediterranean Port of Béjaïa, northeastern Algeria, as indicated by Saadaoui and Bahar (2020). The numerical model assumed has 47 meters high of four horizontal soil layers. Floating stone columns have been installed over a depth of about  $L_c = 19$  meters in a triangular pattern with a distance between axes of  $S_c = 1.60$  meters. Thus, the adopted volume of the unit cell model (UCM) corresponds to a hexagonal cylinder (Fig. 1) of a diameter  $d_e = 1.68$  meters. The phreatic level is 2.50 meters below the upper surface. Due to axial symmetry, only a slice of the unit cell is simulated. The UCM, shown in Fig. 2, adopts a floating stone column of radius  $r_c = 0.40$  meters subjected to different applied pressures ( $q$  varied from 60 kPa to 310 kPa), surrounded by its tributary soil. Therefore, the area replacement ratio is estimated as  $\alpha = 0.22$  ( $\alpha = A_c/A$ ;  $A_c$ : the cross-section of the stone column and  $A$ : the area of the influence zone), and the depth ratio  $\beta = 0.40$  ( $\beta = L_c/H$ ;  $L_c$ : the column length and  $H$ : the thickness of the compressible layer).

Fig. 2 shows the numerical model, the mesh distribution, and the boundary conditions assumed for this analysis. No interface elements are assigned between the floating stone column and the surrounding soil layers. This is due to the fact that no significant shear failure occurs in that zone (Das and Deb, 2019).

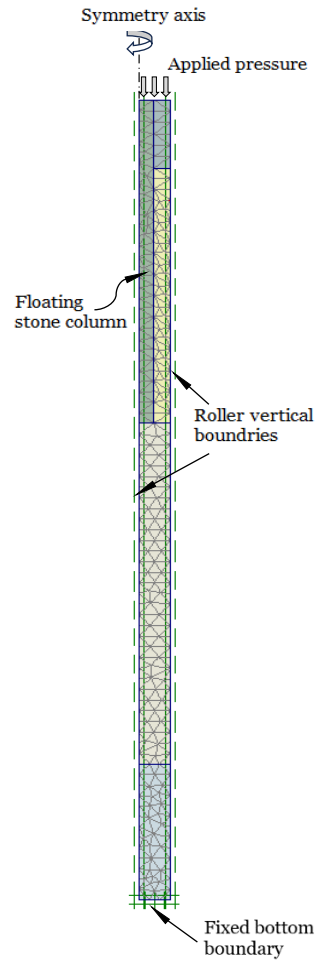


Fig. 2. UCM adopted for the numerical investigation.

The numerical model has the following boundary conditions; vertical displacements are free at the lateral border due to symmetry condition. Additionally, at the bottom level, both horizontal and vertical displacements are fixed (presence of marlstone). The numerical UCM is developed with 15-node triangular elements for mesh generation (Fig. 2). Series of mesh convergence analyses were conducted by changing the global coarseness level to fix the optimum mesh size which gives sufficiently accurate results when compared to the one measured. A very fine mesh without local refinement was assumed for the numerical model. The latter consists of around 6,807 nodes and the total number of elements is equal to 775 with an average size of 0.23 meters. The initial soil and the floating stone column properties, whose characteristics appear in the tables below, Table 1 and Table 2, were derived from the real stone column project in the Port of Béjaïa as indicated by Saadaoui and Bahar (2020). These parameters were obtained through a combination of in-situ recognition tests and laboratory experiments, including granulometric analysis, drained shear tests, oedometer tests, and pressuremeter tests.

Table 1

Characteristics of the initial soil layers.

Parameters	Thickness [m]	$\gamma_s$ [kN/m <sup>3</sup> ]	$\varphi_s'$ [deg]	$c_s'$ [kPa]	$E_s'$ [MPa]	$\nu_s'$ [-]	$\psi_s$ [deg]
Clayey coarse gravel	3.50	15.50	30	1	20	0.33	0
Mud/sandy loams	15.50	15	13	25	6	0.35	0
Grey Muddy-sands	20	16	13	18	8	0.35	0
Marly clay	8	17	23	30	15	0.32	0

**Table 2**

Selected characteristics of the floating stone column employed in the numerical analysis.

Parameters	Length [m]	$\gamma_c$ [kN/m <sup>3</sup> ]	$\phi_c'$ [deg]	$c_c'$ [kPa]	$E_c'$ [MPa]	$\nu_c'$ [-]	$\psi_c$ [deg]
Stone column	19	21	40	1	60	0.33	0

Due to the installation effect of the columns and the improvement of the mechanical properties of the initial soil as well as the confinement provided during the vibro-compaction of the enhancing material, the lateral earth pressure coefficient ( $K$ ), at the vicinity of the floating stone column, is taken equal to 1 (Priebe, 1995). Taking into account the permeable characteristics provided by the closely spaced stone columns, the authors Saadaoui and Bahar (2020) opted for a homogenized permeability value of ( $k$ )  $1.16 \text{ E}^{-4} \text{ m/day}$ .

The linearly elastic-perfectly plastic behavior obeying the Mohr-Coulomb shear failure criterion was considered both for the soil and the stone backfill material. This model, extensively used in geotechnical engineering practice, is still relevant to provide an approximate description of the behavior of granular soils (sands), cohesive soils (including clay and silt soils), and rocks (e.g., Tabchouche et al., 2017). It is relatively simple and requires; the two elastic parameters, namely Poisson's ratio ( $\nu$ ) and Young's modulus ( $E$ ), the two parameters of the Mohr-Coulomb criterion; friction angle ( $\phi$ ) and cohesion ( $c$ ), and the dilatancy angle ( $\psi$ ).

### 2.3. Coupled consolidation analysis

In the computation, a consolidation analysis is performed and the top surface settlement is estimated as a function of time. In *Plaxis<sup>2D</sup>* code, consolidation or drained analysis is conducted according to the theory of Biot for coupled analysis. This theory accounts for the dissipation of excess pore water pressure through either horizontal pore fluid flow from the surrounding soil towards the stone column permitting drainage at the interface, or through vertical fluid flow both leading to volumetric changes with time, as discussed by Das and Deb (2019). Volumetric changes or soil compression under loading, result from the rearrangement of the particles constituting the soil as well as the diminution of the ratio of space occupied by the voids. The time required for the drained analysis is limited to 3120 days (about 9 years) corresponding to the field measurements which were conducted from November 2008 to April 2017 (Saadaoui and Bahar, 2020).

In order for flow and excess pore pressure dissipation to occur, the consolidation boundary conditions are assumed as follows: the right and the left vertical boundaries representing the equivalent diameter limit and the symmetry line respectively, are closed. Also, a closed boundary is applied at the bottom of the UCM at 47 meters depth due to the presence of an impervious layer (a substratum in the form of gray compacted marlstone), while the upper boundary is obviously open.

## 3. Validation of the numerical model

### 3.1. Experimental Validation; in-situ measured data

The long-term settlement obtained from the numerical analysis is compared to that measured from the in-situ settlement response. The stress applied by the structure varies over time until achieving a maximum uniform surcharge of  $q = 310 \text{ kPa}$ . The loading phases applied to the numerical model were evaluated in terms of the increase in the weight of the silo and the load resulting from its storage and charging process, in conformity with the curves of applied stresses in the three-dimensional finite element modeling made by (Saadaoui and Bahar, 2020). In the computation, a uniform surcharge, of 60 kPa, was applied instantly on the top of the numerical UCM in an undrained condition, and then a consolidation analysis was conducted. To simulate the various levels of the silo surcharge, the consolidation analysis comprised the following phases:



- Phase 1:  $q = 60$  kPa from 0 to 400 days;
- Phase 2:  $q = 70$  kPa from 400 to 600 days;
- Phase 3:  $q = 210$  kPa from 600 to 800 days;
- Phase 4:  $q = 255$  kPa from 800 to 1120 days;
- Phase 5:  $q = 260$  kPa from 1120 to 1200 days;
- Phase 6:  $q = 270$  kPa from 1200 to 1320 days;
- Phase 7:  $q = 290$  kPa from 1320 to 3080 days;
- Phase 8:  $q = 310$  kPa from 3080 to 3120 days.

Fig. 3 depicts a time-dependent rate of settlement comparison. The numerical results obtained align well with the field measurements. In the comparative analysis of the two graphs, we initially observe alignment in their behavior for the first 500 days. However, a noticeable deviation occurs as we extend the observation period to 1700 days. The numerical prediction underestimates the settlement with a maximum difference of about 10 centimeters. Beyond this point, the pattern takes a distinct turn, and the predicted settlement remains overestimated, with a maximum value of about 6 centimeters. Finally, a final top surface settlement of 67.5 centimeters was predicted while the measured settlement on April 2017, as indicated by Saadaoui and Bahar (2020), was 66.7 centimeters (relative difference less than  $\pm 1\%$ ). Meanwhile, the immediate settlement predicted by undrained analysis when applying a load of  $q = 310$  kPa is 17.6 centimeters. These results confirm the necessity of taking into consideration the consolidation analysis in the design of floating stone columns.

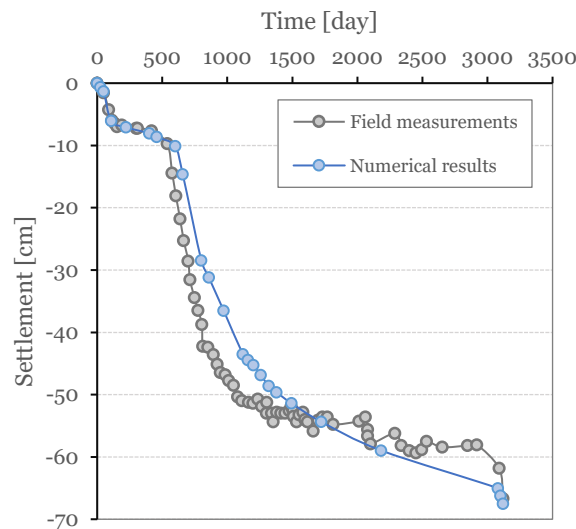


Fig. 3. Comparison of the numerical results with the in-situ records of settlement evolution over time on the top of the central column.

The consolidation settlement plotted as time progresses increases by increasing the loading and leads to heavy damage to the silo. According to Polshin and Tokar (1957), the maximum allowable settlement for solid reinforced concrete foundations of silos is 30 centimeters. It is noteworthy that the long-term settlement recorded on April 2017, 66.70 centimeters, (approximately 10 years after commissioning) exceeds the recommended limitation. This highlights that the design of a group of floating stone columns is governed by the long-term settlement and the maximum applied load. It becomes evident that a group of floating stone columns of 0.80 meters diameter and 19 meters length is insufficient to ensure the stability as well as the durability of the silo since the dissipation period for excess pore pressure towards the drained backfilled material takes time, so that the settlement will be achieved slowly. Finally, assessing the long-term deformation of the improved soil is necessary for a good and effective design of floating stone columns. A proper design leads to accelerating the consolidation of compressible saturated soils, preventing destruction and stability defects.

### 3.2. Analytical validation; Ng and Tan (2014) method

Furthermore, to confirm the validity of the developed model, the consolidation settlement improvement factor predicted is compared to one calculated analytically. A design equation to calculate the final settlement of a group of floating stone columns is proposed by Ng and Tan (2014). The settlement improvement factor,  $n$ , depends on the basic improvement factor,  $n_o$ , and the correction factors,  $C_\alpha$ ,  $C_\varphi$ ,  $C_q$ , and  $C_K$ . It is predicted as:

$$n = n_o [1 - (C_\alpha + C_\varphi + C_q + C_K)] \quad (1)$$

where:

$$n_o = 9.43 \alpha^2 + 1.49 \alpha + 1.06 \quad (2)$$

Based on the selected parameters for the numerical analysis, the correction factors are given in Table 3.

**Table 3**

Correction factors assumed for this analysis (Ng and Tan, 2014).

$C_\alpha, C_\varphi, C_q, C_K$	$\beta$
	0.4
$\alpha = 0.22$	
0.20	0.3302
0.25	0.3978
$\varphi = 40^\circ$	
40°	0
$q = 310 \text{ kPa}$	
250	0.0013
400	0.0017
$K = 1$	
1	-0.0133

After interpolations, the correction factors adopted in the current study are:  $C_\alpha = 0.357$ ,  $C_\varphi = 0$ ,  $C_q = 0.0014$  and  $C_K = -0.0133$ . This calculation yields a settlement improvement factor of  $n = 1.20$  when applying a uniform surcharge equal to  $q = 310 \text{ kPa}$ . The final settlement of the unimproved soil, predicted from the FEM analysis, is 84.0 centimeters. Therefore, the value of the settlement improvement factor is  $n = 1.24$ . It is worth noting that the difference between the results obtained using the numerical method and the method proposed by Ng and Tan (2014) is relatively small, with a negligible relative difference of  $\pm 3\%$ . Since the unreinforced underlying soil layer is deformable, little attention has been devoted to the consolidation beneath the floating stone column which is also important due to the emphasis on the penetration and the submergence of the toe of the floating column in the load transfer, as well as the propagation of shear zones to greater depths (punching failure) (Yang Zhou et al., 2021) (Ng and Tan, 2014) (Weian Liu et al., 2018). Fig. 4 illustrates the incremental shear strains and the plastic points developed beneath the floating stone column toe at the time of 3,120 days.



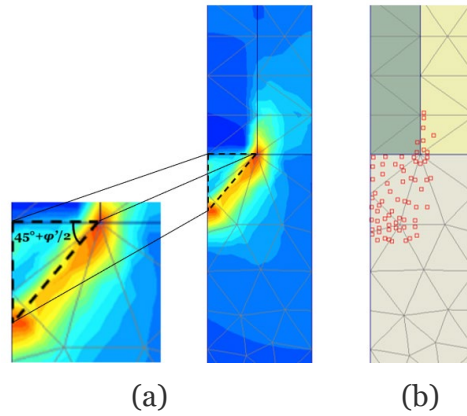


**Fig. 4.** Deformation of the unreinforced underlying layer:

(a) punching shear and (b) plastic points wide spread at the toe of the floating stone column.

As depicted in Fig. 4 (a), the zoomed view of the plane shear failure criteria is similar, as indicated by Ng and Tan (2014), to a circular footing failure plane bounded by two intersected lines; the shear slip line meets the horizontal surface at an acute angle of  $(45^\circ + \varphi'/2)$  (Manoharan and Dasgupta, 1995). At the end of the calculation, the floating stone column toe settles at about 42.2 centimeters due to column punching as well as the unreinforced sub-layer deformation. As noted above, the deformation of the unreinforced underlying layer is significant.

#### **4. Optimized design of floating stone columns group: Application to Algiers Harbor case history (Mole d'El Hadjar)**

##### **4.1. FE model description**

The Algiers Harbor case study in the Algerian capital, is investigated employing the UCM through the two-dimensional finite element program, *Plaxis<sup>2D</sup>*. More details of the unit cell axis-symmetry idealization are described in the section above (2.1). The soil profile of the Mediterranean Port of Algiers adopted for this analysis, has 30 m high of compressible alluvial deposits of silt and clay layers. Three layers of soils are outlined in the profile area. The first upper layer is 1 m thick of muddy-sands with gravel. The second sub-layer varies in thickness from 10 to 15 meters and consists of silty muddy-sands. And the third sub-layer is 14 meters of marly clay. The ground water level (G.W.T) is situated at a depth of 1.94 meters. The initial soil properties used in this study were obtained through a comprehensive site investigation program, which involved a series of tests, including standard penetration tests (SPT), Cone Penetration Tests with pore pressure measurement (CPTu), and laboratory tests such as oedometer and triaxial tests.

The project focuses on the management of the platform of the Port of Algiers (potentially liquefiable and deformable) which supports an overload of  $q = 55$  kPa applied on a strip footing of width of  $B = 16.38$  meters supporting 7 rows of containers of 40 feet (Mehenni and Boulifa, 2017). Initially, a large group of end-bearing stone columns of a diameter of  $D_c = 1.20$  meters is adopted. However, the column length,  $L_c$ , depends on the extent of the compressible muddy-sands layer, which, as per the geotechnical profiles, ranges from 10 meters to 16 meters. The floating stone columns are arranged in the more commonly practiced grid; equilateral triangular pattern, and the equivalent diameter was calculated as  $d_e = 2.10$  meters. The area improvement ratio is, then, determined as  $\alpha = 0.33$ . Fig. 5 shows the adopted arrangement pattern of the floating stone columns.

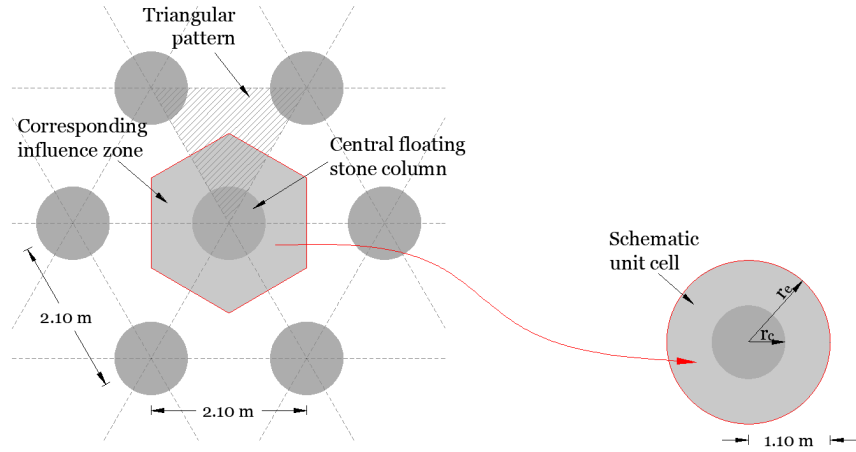


**Fig. 5.** The adopted floating stone columns arrangement and the corresponding equivalent circle.

For all numerical computations, 15-node triangular elements were discretized. Coarse, medium, fine and very fine mesh were tested to adopt the adequate mesh size. A very fine mesh was assumed. The Mohr-Coulomb constitutive law is adopted. The boundary conditions of the built UCM are: roller boundaries for both left and right sides, and both horizontal and vertical displacements are fixed at the base level of the UCM. Fig. 6 shows the numerical unit cell model of the Port of Algiers case study.

The initial soil and the floating stone column material parameters examined in the current numerical analysis are recapitulated in Table 3 and Table 4.

**Table 3**

Material properties for the unit cell model (after Mehenni and Boulifa, 2017).

Parameters	Thickness [m]	$\gamma_d$ [kN/m <sup>3</sup> ]	$\phi_s'$ [deg]	$c_s'$ [kPa]	$E_s'$ [MPa]	$\nu_c'$ [-]	$\psi_s$ [deg]	$k$ [m/day]
Muddy-sands with gravel	1	16.68	32	1	5.50	0.27	0	$8.64 \text{ E}^{-4}$
Silty Muddy-sands	15	17.66	32	1	5.50	0.27	0	$8.64 \text{ E}^{-2}$
Marly clay	14	15.20	27	35	26	0.30	0	$1.50 \text{ E}^{-5}$

**Table 4**

Selected parameters of column coarse backfill material (after Mehenni and Boulifa, 2017).

Parameters	Length [m]	$\gamma_d$ [kN/m <sup>3</sup> ]	$\phi_c'$ [deg]	$c_c'$ [kPa]	$E_c'$ [MPa]	$\nu_c'$ [-]	$\psi_c$ [deg]	$k$ [m/day]
Stone column	10-16	21	40	1	60	0.33	0	1

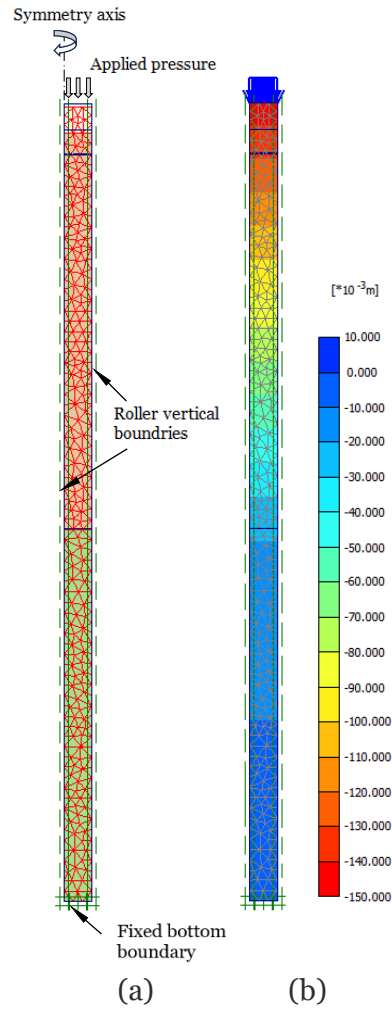


Fig. 6. Boundary conditions and generated mesh distribution of UCM simulated in *Plaxis*<sup>2D</sup>: (a) deformed mesh and (b) settlement contours.

#### 4.2. Comparison with Ng and Tan (2014) analytical method

As there were limited experimental data and limited tests on the stone column, finite element verification was conducted using Ng and Tan (2014) analytical solution. The comparison was conducted with an end-bearing stone column of a length of 16 meters ( $\beta = 1$ ). The analytical calculation yields a settlement improvement factor of  $n = 2.58$ . On the flip side, the FEM analysis predicts a final settlement of the unimproved soil to be 15 centimeters, aligning precisely with the measurement taken in August 2004 (DTP; public works department of Algiers). Conversely, the final settlement of the improved soil is 5.8 centimeters. Consequently, the settlement improvement factor, denoted as  $n$ , stands at 2.55, reflecting a relative difference of approximately  $\pm 1\%$ .

#### 4.3. Overview of parametric analysis

One of the frequently encountered challenges in the conception of floating stone columns groups is determining the optimized design to avoid higher volume substitution and over costs. On the grounds of this and to examine the impact of floating stone column geometric variables on the composite system behavior (soil-column), coupled finite element analyses were conducted with the developed numerical UCM to analyze the impact of the area improvement ratio,  $\alpha$ , and the column length,  $L_c$ , i.e., the depth substitution ratio, on the total allowable settlement under both undrained and drained conditions. The area replacement ratio was

varied as currently practiced in the vibro-replacement technique which is found to lie between 0.10 and 0.33 (e.g., Bouassida, 2016). Besides, the floating stone column length was varied from  $L_c = 2$  meters to  $L_c = 16$  meters. In total, 48 models have been undertaken in order to provide a detailed analysis.

According to Skempton and MacDonald (1956) the maximum settlement allowed for rafts founded on sandy soils to settle is estimated at 7 centimeters (2 to 3 inches). The authors collected a data-records of ninety-eight (98) buildings, of which 40% have been damaged as a consequence of settlement. The purpose of this analysis was to suggest limits for the total and the differential settlements of several types of foundations. Therefore, the proposed design should adhere to the admissible deformation limit, which must be equal to or less than 7 centimeters.

### 4.3 Results and discussion

#### 4.4.1 Undrained analysis

The immediate settlement predictions for various area replacement ratios and the column lengths are summarized in Table 5.

**Table 5**

Short-term settlement.

Settlement [cm]		$\alpha$					
		0.10	0.15	0.18	0.23	0.27	0.33
$L_c$ [m]	2	12.20	11.90	11.90	11.80	11.80	11.70
	4	11.80	11.30	11.20	11.00	10.90	10.70
	6	11.40	10.70	10.50	10.10	9.90	9.60
	8	10.90	10.10	9.60	9.20	8.90	8.50
	10	10.40	9.40	8.90	8.30	7.80	7.30
	12	9.90	8.70	8.00	7.30	6.70	6.10
	14	9.40	7.80	7.10	6.20	5.60	5.00
	16	8.70	7.00	6.10	5.10	4.40	3.70

Fig. 6 indicates that as the volume substitution,  $\alpha$ , and  $L_c$ , increases, the settlement reduces, while the improved ground of the floating stone column led to a reduction in the settlement to 3.70 centimeters for  $\alpha = 0.33$  and  $L_c = 16$  meters. However, for this design, the substantial amount of backfilled ballast significantly contributes to the overall high cost, casting a negative light on the technique. Nevertheless, it must be acknowledged that despite this drawback, this technique of improvement still remains cost-effective compared to alternative techniques.

The limiting maximum settlement, which cannot be safely exceeded, is gained when  $\alpha = 0.15$  for  $L_c = 16$  meters,  $\alpha = 0.18$  for  $L_c = 14.20$  meters,  $\alpha = 0.23$  for  $L_c = 12.60$  meters,  $\alpha = 0.27$  for  $L_c = 11.50$  meters and  $\alpha = 0.33$  for  $L_c = 10.50$  meters.

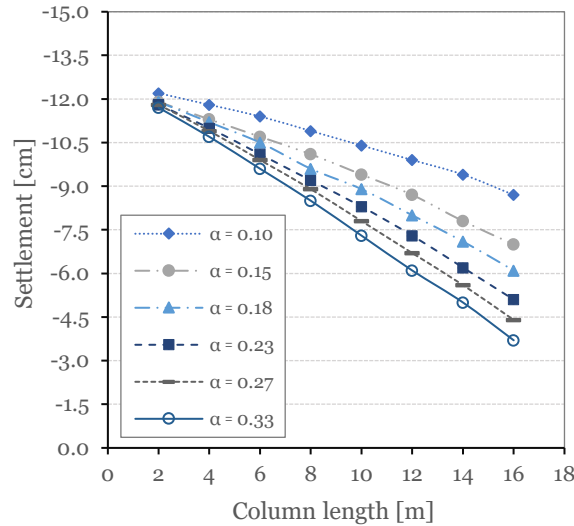


Fig. 6. Effect of  $\alpha$  and  $L_c$  on short-term settlement.

Since the cost of vibro replacement is essentially controlled by the volume fraction of the incorporated coarse material in reference to the improvement surface ratio, an end-bearing column of 16 meters length with an area substitution of  $\alpha = 0.15$  is a suitable optimized design in short-term condition since the settlement predicted equals the admissible limitation. The present analysis does not consider the possible influence of the strip footing width, which would require a 3D analysis.

#### 4.4.2 Drained analysis (Consolidation)

Devoting attention to the optimized design of floating stone columns in long-term conditions involves studying the effect of the area improvement ratio and the floating column length on the allowable consolidation settlement, ultimately resulting in the final optimized design. A summary of the final consolidation settlements is presented in Table 6.

Table 6

Final consolidation settlement.

Settlement [cm]		$\alpha$					
		0.10	0.15	0.18	0.23	0.27	0.33
$L_c$ [m]	2	14.32	14.04	14.04	13.95	13.92	13.86
	4	13.96	13.49	13.33	13.16	13.02	12.84
	6	13.56	12.93	12.64	12.31	12.04	11.78
	8	13.08	12.23	11.83	11.44	11.04	10.62
	10	12.58	11.53	11.05	10.46	9.94	9.47
	12	12.04	10.82	10.18	9.44	8.89	8.28
	14	11.47	10.02	9.24	8.40	7.72	7.13
	16	10.81	9.41	8.16	7.29	6.53	5.88

The numerical analysis illustrates that the final consolidation settlement exceeds the allowable limit when adopting end-bearing stone columns and area substitution ratios of  $\alpha = 0.10$ ,  $\alpha = 0.15$ ,  $\alpha = 0.18$  and  $\alpha = 0.23$ . However, the maximum allowable settlement is still achieved even when the stone columns are not fully penetrated ( $\beta = 1$ ). This occurs when  $\alpha = 0.27$  for  $L_c = 15.20$  meters and  $\alpha = 0.33$  for  $L_c = 14.20$  meters. The optimized designed for this case would be end-bearing columns ( $L_c = 16$  m) with  $\alpha = 0.25$  or floating columns of  $\alpha = 0.27$  for  $L_c = 15.30$  meters and  $\alpha = 0.33$  for  $L_c = 14.20$  meters. It is evident that these results clearly diverge from those obtained in the undrained analysis. When compared to the optimized design, this

emphasizes the significance of taking long-term behavior into account in the design of floating stone columns.

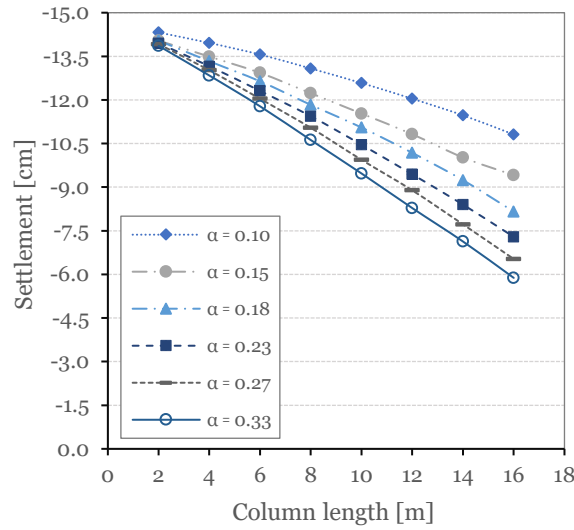


Fig. 7. Effect of  $\alpha$  and  $L_c$  on the final consolidation settlement.

It is evident, furthermore, that an increase in both the area substitution ratio and the length of the floating column results in a reduction of the final consolidation settlement. As indicated, from Fig. 7, the deeper is the depth substitution, the lower is the final consolidation settlement. However, contrary to the area substitution ratio, the column length has less importance on the performance in terms of reducing the settlement. In relation to this, for  $\alpha = 0.10$ , increasing the floating column length from 2 meters to 16 meters leads to reducing the final consolidation settlement by only 25% (Fig. 8). In contrast, for  $\alpha = 0.33$  the final consolidation settlement drops by 60% (Fig. 8). Nevertheless, this impact is less noticeable when the column is of shorter length and the performance is nearly identical for a small area improvement ratio. The relative difference in the final consolidation settlement when  $\alpha = 0.33$  and  $\alpha = 0.10$  for  $L_c = 2$  m is approximately  $\pm 3.26$  %. This is primarily due to the fact that the unimproved compressible layer exerts a dominant influence on the behavior and the consolidation process of the entire system. As a result, it can be deduced that the variation in the area improvement influences both the magnitude of the deformation and the optimum length of the floating stone column.

These results with regard to the impact of the area substitution and the length of the floating stone column is in good agreement with the work of Beyene et al. (2023), in which an interrelationship between the consolidation settlement and drains dimension was reported. The consolidation settlement plotted over time for  $\alpha = 0.10$  and  $\alpha = 0.33$  is presented in Fig. 8.



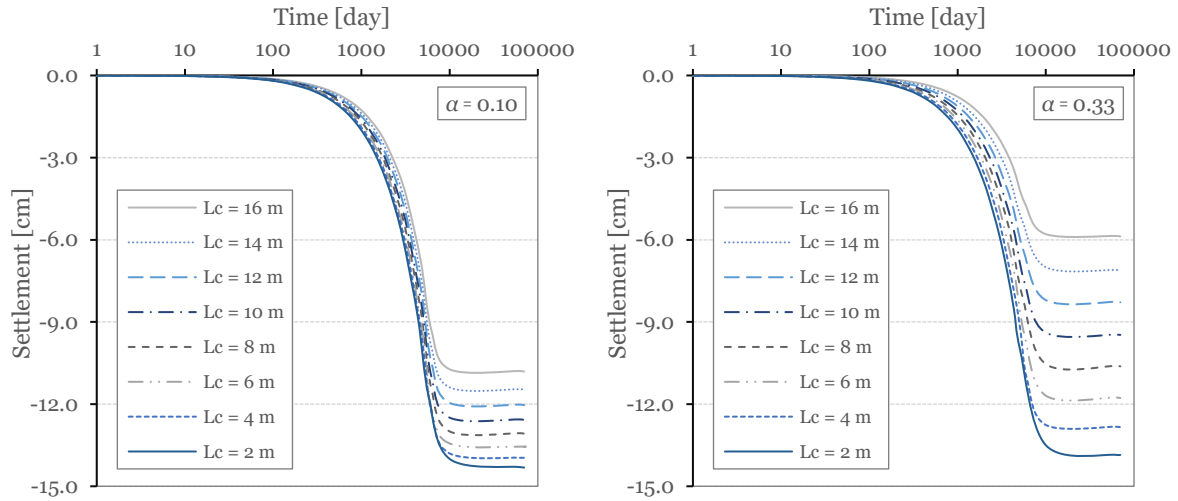


Fig. 8. Final consolidation settlement for different column lengths.

The analysis is extended to investigate the load level as it exerts a crucial influence on the design of floating stone columns. For this reason, loading was applied in 25 kPa increments, reaching a level of 175 kPa. This investigation aimed to assess its significance in the design of a large group of floating stone columns. Fig.9 shows that as the load level increases, the final settlement increases. In essence, the higher the load level, the more demanding the design requirements become to ensure proper settlement control and stability.

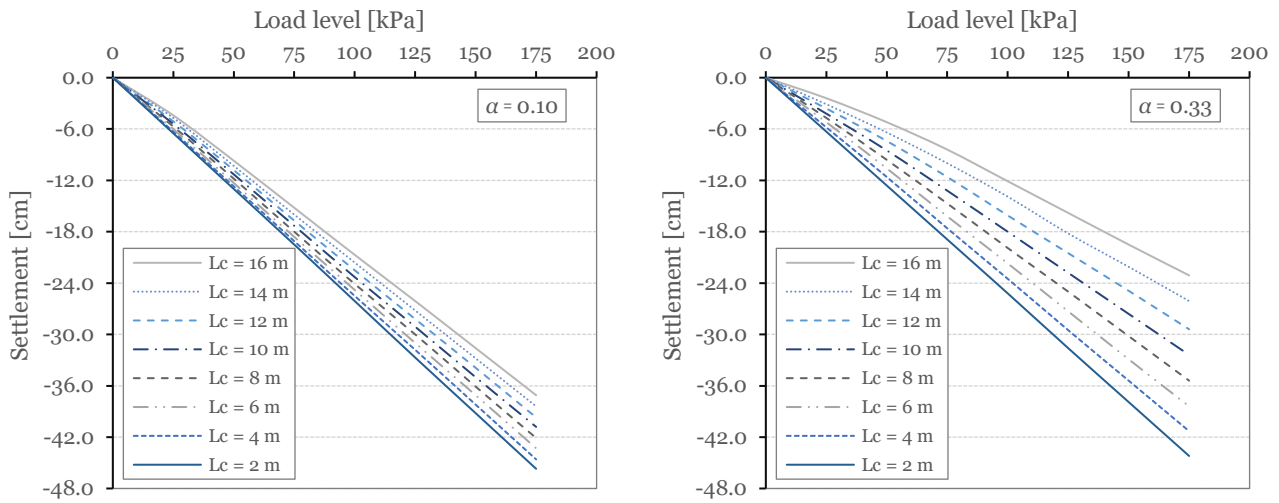


Fig. 9. Influence of load level.

## 5. Conclusions

Numerical investigations using 2D finite element analyses of a unit cell model have been performed to analyze the impact of different geometric design variables, namely; area improvement ratio and length, on soft soil stabilization in terms of settlement, being indispensable for optimizing the design of floating stone columns. Considering the numerical findings, the following conclusions can be drawn:

- 1- The primary performance is not sufficient for the design of a large group of floating stone columns; compressible fully saturated soft soils, often exceeding 20 meters in thickness, are characterized by low permeability leading to slow rates of consolidation and poor water dissipation, causing long-lasting excessive settlement problems once loaded. Therefore, it is essential to consider consolidation analysis for an effective

design, as designs based on immediate settlement do not usually align with long-term behavior.

- 2- The effect of the area improvement ratio is more significant than the column's length; as the area substitution increases, the optimal length decreases. Nevertheless, this impact is less prominent when the column is of shorter length and is nearly identical for a small area improvement ratio. This is primarily due to the fact that the unimproved compressible thick layer exerts a dominant influence on the behavior and the consolidation process of the entire system. Consequently, it can be deduced that the variation in the area improvement affects both the magnitude of the deformation and the optimal length of the floating stone column.
- 3- Without a proper evaluation of the maximum applied stress, the output of the design is flawed; the design of floating stone columns is highly dependent on the pressure exerted by the construction; the examination of the load level impact on stone column design revealed that assessing the load level is of the utmost importance in the design process.

## References

- Beyene, A., Merka, H., & Tsige, D. (2023). Suitability analysis of vertically installed scoria gravel drains for enhancing consolidation performance of clayey ground. *Results in Engineering*, 17, 100975.
- Boru, Y. T., Negesa, A. B., Scaringi, G., & Puła, W. (2022). Settlement analysis of a sandy clay soil reinforced with stone columns. *Studia Geotechnica et Mechanica*, 44(4), 333-342.
- Shehata, H. F., Sorour, T. M., & Fayed, A. L. (2021). Effect of stone column installation on soft clay behavior. *International Journal of Geotechnical Engineering*, 15(5), 530-542.
- Miranda, M., Fernández-Ruiz, J. & Castro, J. (2021). Critical length of encased stone columns. *Geotextiles and Geomembranes* 49 (5), 1312-1323.
- Bouassida M, Guetif Z (2000) Etude comparative : Pieux- Colonnes : cas du siège des chèques postaux à Tunis. Séminaire sur le renforcement des sols : Etat de l'art et perspectives en Tunisie, ENIT – BP 37, Le Belvédère 1002 Tunis. pp. 65-78.
- Tabchouche, S. and Bouassida, M. (2020). Lateral expansion of granular piles under vertical loading: Numerical and experimental investigation Proc. 4th Int. Conf. Geotech. Engineering, 9-10 March 20, Hammamet, Tunisia. Edit. Karoui et al, 179-185.
- Impe, V. (1983). Improvement of settlement behaviour of soft layers by means of stone columns. In *Proceedings, 8th European Conference on Soil Mechanics and Foundation Engineering: Improvement of Ground, Helsinki* (Vol. 1, p. 309).
- Schweiger, H. F., & Pande, G. N. (1986). Numerical analysis of stone column supported foundations. *Computers and Geotechnics*, 2(6), 347-372.
- Mitchell, J. K., & Huber, T. R. (1985). Performance of a stone column foundation. *Journal of Geotechnical Engineering*, 111(2), 205-223.
- Castro, J. (2017). Modeling stone columns. *Materials*, 10(7), 782.
- Castro, J., & Sagaseta, C. (2011). Consolidation and deformation around stone columns: Numerical evaluation of analytical solutions. *Computers and Geotechnics*, 38(3), 354-362.
- Castro, J., Karstunen, M., & Sivasithamparam, N. (2014). Influence of stone column installation on settlement reduction. *Computers and Geotechnics*, 59, 87-97.

- Doan, S., & Fatahi, B. (2020). Analytical solution for free strain consolidation of stone column-reinforced soft ground considering spatial variation of total stress and drain resistance. *Computers and Geotechnics*, 118, 103291.
- Ng, K. S., & Tan, S. A. (2014). Design and analyses of floating stone columns. *Soils and Foundations*, 54(3), 478-487.
- Bouassida, M. (2016). *Design of column-reinforced foundations* (Vol. 240). Plantation: J. Ross Publishing.
- Imam, R., Zarei, M., & Ghafarian, D. (2021). Relative contribution of various deformation mechanisms in the settlement of floating stone column-supported foundations. *Computers and Geotechnics*, 134, 104109.
- Priebe, H. J. (1976). Evaluation of the settlement reduction of a foundation improved by Vibro-Replacement. *Bautechnik*, 2, 160-162.
- Priebe, H. J. (1995). The design of vibro replacement. *Ground engineering*, 28(10), 31.
- Ellouze, S., Bouassida, M., Hazzar, L., & Mroueh, H. (2010). On settlement of stone column foundation by Priebe's method. *Proceedings of the Institution of Civil Engineers-Ground Improvement*, 163(2), 101-107.
- Remadna, A., Benmebarek, S., & Benmebarek, N. (2020). Numerical analyses of the optimum length for stone column reinforced foundation. *International Journal of Geosynthetics and Ground Engineering*, 6, 1-12.
- Killeen, M. M., & McCabe, B. A. (2014). Settlement performance of pad footings on soft clay supported by stone columns: a numerical study. *Soils and Foundations*, 54(4), 760-776.
- Elshazly, H. A., Hafez, D. H., & Mossaad, M. E. (2008). Reliability of conventional settlement evaluation for circular foundations on stone columns. *Geotechnical and Geological Engineering*, 26, 323-334.
- Balaam, N. P., & Booker, J. R. (1981). Analysis of rigid rafts supported by granular piles. *International journal for numerical and analytical methods in geomechanics*, 5(4), 379-403.
- Wang, G. (2009). Consolidation of soft clay foundations reinforced by stone columns under time-dependent loadings. *Journal of geotechnical and geoenvironmental engineering*, 135(12), 1922-1931.
- Nayak, S., Vibhoosha, M. P., & Bhasi, A. (2019). Effect of column configuration on the performance of encased stone columns with basal geogrid installed in lithomargic clay. *International Journal of Geosynthetics and Ground Engineering*, 5, 1-19.
- Sadaoui, O., & Bahar, R. (2020). Analyse numérique et expérimentale du comportement des ouvrages fondés sur un sol mou renforcé par des colonnes ballastées flottantes. *Bulletin of Engineering Geology and the Environment*, 79, 2721-2745.
- Das, A. K., & Deb, K. (2019). Response of stone column-improved ground under c- $\phi$  soil embankment. *Soils and Foundations*, 59(3), 617-632.
- Tabchouche, S., Mellas, M., & Bouassida, M. (2017). On settlement prediction of soft clay reinforced by a group of stone columns. *Innovative Infrastructure Solutions*, 2, 1-12.
- Polshin, D. E., & Tokar, R. A. (1957, August). Maximum allowable non-uniform settlement of structures. In *Proc., 4th Int. Conf. on Soil Mechanics and Foundation Engineering* (Vol. 1, pp. 402-405). London: Butterworth's.
- Zhou, Y., Kong, G., Wen, L., & Yang, Q. (2021). Evaluation of geosynthetic-encased column-supported embankments with emphasis on penetration of column toe. *Computers and Geotechnics*, 132, 104039.
- Liu, W., & Hutchinson, T. C. (2018). Numerical investigation of stone columns as a method for improving the performance of rocking foundation systems. *Soil Dynamics and Earthquake Engineering*, 106, 60-69.

- Manoharan, N., & Dasgupta, S. P. (1995). Bearing capacity of surface footings by finite elements. *Computers & structures*, 54(4), 563-586.
- Skempton, A. W., & MacDonald, D. H. (1956). The allowable settlements of buildings. *Proceedings of the Institution of Civil Engineers*, 5(6), 727-768.
- Hammad, M. S., Fayed, A. L., & El-Mossallamy, Y. M. (2019). Application of prefabricated vertical drains in soft clay improvement. *International Journal of Engineering and Applied Sciences*, 6(10), 68-77.
- Radhakrishnan, G., Raju, G. V. R., & Venkateswarlu, D. (2010, December). Study of consolidation accelerated by sand drains. In *Indian Geotechnical Conference* (pp. 16-18).
- Mehenni, M.A., and Boulifa, W. (2017). Amélioration de sol du port d'alger par colonnes ballastées (Master's thesis, University Of Science and Technology Houari Boumediene).